Princeton Plasma Physics Laboratory

PPPL- 4661

PPPL- 4661

Cross-Field Electron Transport Induced By A Rotating Spoke In A Cylindrical Hall Thruster

C.L. Ellison, Y. Raitses and N.J. Fisch

August, 2011

Prepared for the U.S. Department of Energy under Contract DE-AC02-09CH11466.

Princeton Plasma Physics Laboratory
Report Disclaimers

Full Legal Disclaimer

Trademark Disclaimer

PPPL Report Availability

Princeton Plasma Physics Laboratory:

http://www.pppl.gov/techreports.cfm

Office of Scientific and Technical Information (OSTI):

http://www.osti.gov/bridge

Related Links:

U.S. Department of Energy

Office of Scientific and Technical Information

Fusion Links

Cross-field electron transport induced by a rotating spoke in a cylindrical Hall thruster

C. L. Ellison, Y. Raitses, N. Fisch

Princeton Plasma Physics Laboratory, Princeton, NJ 08543

(Dated: 17 August 2011)

Rotating spoke phenomena has been observed in a variety of Hall thruster and other $\mathbf{E} \times \mathbf{B}$ devices. It has been suggested that the spoke may be associated with the enhancement of the electron cross-field transport. In this paper, the current conducted across the magnetic field via a rotating spoke has been directly measured for the first time in the $\mathbf{E} \times \mathbf{B}$ of a cylindrical Hall thruster. The spoke current was measured using a segmented anode. Synchronized measurements with a high speed camera and a four-segment anode allow observation of the current as a function of azimuthal position. Upwards of 50% of the total current is conducted through the spoke, which occupies a quarter of the Hall thruster channel. To determine the transport mechanism, emissive and Langmuir probes were installed to measure potential and density fluctuations (respectively). An azimuthal electric field and density fluctuations are observed to oscillate in-phase with the rotating spoke. A contributing transport mechanism is proposed to be an axial $\mathbf{E} \times \mathbf{B}$ electron drift towards the anode caused by the perturbed azimuthal electric field.

I. INTRODUCTION

Cross-field transport is of fundamental interest in a variety of devices, including magnetically confined fusion plasmas, Penning traps, magnetrons, and Hall thrusters[1–4]. In addition to classical collisional transport, electron mobility may be enhanced by electron-wall interactions[5], fluctuations[6–9], and turbulence[10].

In the Hall thruster, cross-field transport is of practical importance because it diminishes the thruster efficiency. Hall thrusters typically consist of an annular channel in which a radial magnetic field confines electrons, while an axial electric field accelerates ions. A cathode neutralizer maintains neutrality throughout the plasma, mitigating space charge limitations present in other plasma thrusters. A higher specific impulse compared to electrothermal thrusters and larger thrust-per-mass ratio compared to electrostatic ion thrusters makes Hall thrusters preferable candidates for orbital correction and light-weight space missions, such as the SMART-1 European Space Agency mission[11].

While annular Hall thrusters have successfully operated in the kW power range, the cylindrical Hall thruster (CHT) has been proposed for efficient scaling to low (100-200 W) power levels[12]. In this configuration, the central portion of the annular channel is eliminated, forming a mirror field within a cylindrical channel. The electrons are confined on the near-anode side by the mirror force and on the cathode side by the axial electric field. The decreased surface area of the cylindrical shape is intended to enhance performance by minimizing electron-wall interactions. Like the annular Hall thruster, the CHT exhibits anomalous levels of cross-field transport[13].

A rotating spoke of light has been observed in annular[14–17] and cylindrical[18] Hall thruster geometries, as well as in more general $\mathbf{E} \times \mathbf{B}$ devices[19]. Early studies used electrostatic probes to measure fluctuating density and potential, and inferred the spoke to be contributing to the anomalous transport[14]. The magnitude of the fluctuations appeared to be on the correct order to explain the anomalously high levels. A similar use of emissive probes have observed rotation in a more recent study[20], though the measurements were performed at low discharge voltage (200 V) and the unclear azimuthal behavior combined with a counter-$\mathbf{E} \times \mathbf{B}$ rotation direction make comparisons with past results difficult. Imaging of annular thruster ignition has revealed azimuthal behavior which may also be related to the rotating spoke[21].

Recently, Parker et al. observed a 15-35 kHz rotating spoke on the cylindrical Hall thruster using a fast camera and electrostatic probe diagnostics[18]. A series of fast camera images is shown in Fig. 1, showing the characteristic azimuthal rotation of the spoke. The spoke was found to rotate in the $\mathbf{E} \times \mathbf{B}$ direction with a speed of 1.2 - 2.8 km/s, which is substantially less than the local E/B speed of 30 km/s. In-channel Langmuir probes indicated the strongest correlation between density fluctuations and light emissions was near the anode. By increasing the cathode keeper current, which controls the electron supply to the thruster discharge[22], a transition to high-frequency oscillations replaced the spoke behavior. The cross-field electron transport, characterized by the ratio of the discharge current to the expelled ion current, was observed to decrease when the spoke oscillation was suppressed, suggesting the spoke was altering the cross-field transport. It is then hypothesized that the oscillation mechanism responsible for the rotating light spoke also enhances the local current to the anode.

The similarities of these[14–18,20] findings (with the possible exception of Ref.[20]), including an azimuthal perturbation rotating in the $\mathbf{E} \times \mathbf{B}$ direction with a frequency of 10-35 kHz and a velocity slower than the E/B speed, lead us to suggest the phenomena are related. In this paper, we demonstrate the mechanism of the rotating spoke does alter the cross-field electron transport. Preliminary findings using a segmented anode were presented in Ref.[23]. The cross-field current induced by the spoke is directly measured for the first time by installing a segmented anode. Typically, oscillations in the discharge current are monitored, but a continuous anode can only observe longitudinal oscillations, such as the ionization breathing mode. A rotating spoke which conducts current would only enhance the current locally (in the azimuthal direction), and thus maintain a constant discharge current. By separating the anode into four azimuthal segments, the current may be observed as a function of position. Measuring the current to each segment in time, synchronized with the fast camera, allows direct identification of the spoke-induced cross-field current. Indeed, we find over half of the total current traverses the rotating spoke, which is large considering the spoke occupies $\sim$25% of the channel area. To supplement the identification of enhanced cross-field current, the transport mechanism is investigated using emissive and Langmuir probes to determine the phase of the fluctuating potential and density relative to the phase of the spoke. The spoke is determined to possess an azimuthal electric field, and a quantitative estimate is provided of the axial electron drift contribution to the enhanced current.

II. METHODS

The experiments were performed at the Large Hall Thruster facility at the Princeton Plasma Physics Laboratory, as described elsewhere[24]. The vacuum vessel is equipped with cryogenic pumps and the background pressure does not exceed 3 μtorr during operation. The basic schematic for the 2.6 cm diameter CHT is shown in Fig. 2[24]. Typical operating parameters include a 4 cm^3/s at standard temperature and pressure (sccm) xenon mass flow to the anode, 2 sccm xenon flow to the cathode, 250 V discharge voltage, 2.5 A for the back coils and -2.0 A for the front coils. The opposite polarity of the fields forms a magnetic cusp near the channel exit and enhances the radial field, as shown in Fig. 3. The field strength near the anode is 850 G. The hollow cathode was operated with a keeper current, I_k, of 1.5 - 1.8 A. Keeper current is a significant parameter, given the wide variety of oscillatory behavior observed for different settings[18,22]. By enhancing the electron emission from the cathode, the ionization-based breathing mode may be suppressed. Given the close frequency of the breathing mode and rotating spoke, suppression of the breathing mode simplifies analysis by ensuring the dominant oscillation in the low frequency range is the rotating spoke. At higher keeper current (3.0 A), the spoke oscillation is also suppressed and high frequency (MHz) oscillations appear. A 1.5 A keeper current has been found to be a satisfactory mid-range value for clear spoke observation.

A Vision Research Phantom v7.3 fast camera has been used extensively while studying the rotating spoke. The camera is capable of up to 500,000 frames per second (fps), though typical spoke observations were performed near 200 kfps to achieve a resolution of 64x64 pixels. Observations are made 7 m from the thruster and along the axis.

Whereas previous configurations[18,24] have used a combined anode and gas distributor, the apparatus for this experiment uses distinct anode and gas distribution components. Two gas inlet tubes extend from the rear of the thruster to the gas distributor positioned behind the anode. Many small holes extend radially from within the gas distributor to provide uniform xenon distribution around the anode. The segmented anode is shown in Fig. 4. A boron nitride base electrically isolates the four anode segments from the gas distributor. The holes around the outer and inner diameter allow the gas to reach the channel from the distributor. The anode segments are 21.6 mm from the channel exit. A single power supply applies the discharge voltage (typically 250 V) between the segmented anode and the hollow

cathode, positioned several centimeters beyond the thruster exit. 1 Ω resistors in series with each segment allow measurement of the current.

A primary concern was verifying the segmented anode did not alter the operation of the CHT. Impeded gas flow, uncertainties in the axial location of the anode and modified surface behavior could alter thruster performance. Proper thruster performance was confirmed by comparing characteristic parameters and transitions in oscillation regimes. Indeed, the total discharge current was observed to be 0.85 A, which is typical for this thruster with the cusp field configuration. Similarly, the transitions in breathing mode, spoke, and high frequency oscillations were obtained by modifying the cathode keeper current, and the behavior matched that of previous studies[18]. To confirm no current was being collected by the gas distributor, an attempt was made to start the thruster while biasing the gas distributor instead of the segmented anode. The thruster would not ignite. These verifications suggest that the thruster behavior and ultimately rotating spoke behavior are unaltered by the segmented anode.

One detriment to the segmented anode operation was a dielectric coating which appeared on the anode over time. The presence of an anode coating is not new[25,26], but can be important when considering the time response of the segments. After several hours of operation, the coating could be observed as discoloration on the stainless steel, and care was taken to remove the coating between experimental efforts. The visual characteristics were similar to those described in Ref.[26], including blue-green and brown hues. Past studies concluded the composition of the dielectric to be oxides of the apparatus, such as stainless steel. The addition of a capacitive component could add a phase delay to the signal, but the 4 - 7 μs between camera frames is longer than any observed delays. However, care was taken to clean the dielectric coating between experiments to ensure the four segments behaved equally.

For the electrostatic probe measurements, 12 radial holes extend at 4 azimuthal positions and 3 axial positions for probe insertion as can be seen in Fig. 5. The probes are centered above each segment to directly relate the probe signals to the local current. For this set of experiments, emissive probes were placed at the 2 o'clock and 11 o'clock positions while Langmuir probes were placed at the 5 and 8 o'clock positions (as viewed by the fast camera). The axial location of all probes is 5 mm from the anode since previous work determined the spoke to reside near the anode[18] and the fluctuations at this position will most directly

relate to the anode current.

The emissive probes extrude a thoriated tungsten filament 1mm x 0.5mm into the plasma while the Langmuir probes are positioned flush with the channel wall with an area of 1 mm^2. The emissive probe was heated until additional increase in the current did not increase the floating potential. Visible emission from the probe further confirmed it to be operating in the 'strongly emitting' regime. Recent measurements indicate the emissive probe floats nearly 2 electron temperatures below the plasma potential[27], as may be expected in the presence of a space-charge saturated sheath[28]. The Langmuir probes were biased +48 V above ground to operate in the ion saturation current regime, which is a negative bias compared to the 175 V - 200 V space potential. Plasma density as a function of time was calculated using the ion saturation current to the planar probe, using the expression for the Bohm ion flux at the sheath edge as follows:

$$I_{sat} = 0.6 q_e n_e A c_s \tag{1}$$

Where q_e is the electron charge, n_e the electron density in the bulk plasma, A the probe area, and c_s is the ion sound speed. The electron temperature is taken to be 16 eV as identified in previous CHT studies[29]. Equation 1 assumes a small, planar sheath compared to the probe dimensions and takes the ions to be drifting to the biased probe with the Bohm velocity while repelling all electrons. All signals were digitized using LeCroy Waverunner 350 MHz and 500 MHz oscilloscopes. A function generator was used to trigger the fast camera and oscilloscopes.

Probe measurements inside the channel must be performed carefully to prevent perturbing the plasma environment[30]. Biasing the Langmuir probe at the wall alters the floating sheath geometry and collects particles which would otherwise be in the plasma. The extruding emissive probe extends into the bulk of the plasma, and (despite floating) can alter the electron distribution function through emissions. Emissive probes are also delicate and may be quickly be destroyed in the harsh plasma. Probe measurements were possible because of the near-anode axial location, as has been achieved in previous studies[28,29]. This region is before the acceleration zone, and thus the plasma is less likely to harm the probes and thruster operation will be less sensitive to small space potential perturbations. The discharge current remained near 0.85 amps, even with the emitting probes and while collecting ion saturation current. To test for azimuthal perturbations, we measured the floating potential

of a probe directly adjacent to the emitting probe in the in the $\mathbf{E} \times \mathbf{B}$ direction. The floating potential showed no change with the probe emitting or cold, confirming no significant perturbation to the steady state potential. It is interesting to note that comparison of the spoke potential with the location of enhanced light emission is greatly aided by the segmented anode. During the probe emission, the bright light from the probe makes visible imaging of the rotating spoke difficult. Given the large correlation between the visible light and the measured current (see section III), the segmented anode currents may be used to identify the location of the rotating spoke when probe emissions hinder fast camera imaging.

III. RESULTS

The fast camera, segmented anode, and electrostatic probes allowed direct measurements of the cross-field current conducted through the rotating spoke for the first time. The spoke was found to enhance the current as camera and segmented anode measurements indicate over half of the total current traverses the spoke. Observations of the density and potential fluctuations supplement the current measurements by suggesting properties of the transport mechanism. The breathing mode was successfully suppressed using enhanced cathode keeper current, isolating the rotating spoke as the dominant oscillation. Electrostatic probe measurements near the anode provided more detailed measurements of the phenomena, providing characteristic density and potential fluctuations relative to the enhanced current. The phase of the density and potential relative to the spoke current indicate a perturbed electron drift towards the anode. As a simple qualitative model of the transport mechanism, a drift current was estimated using the perturbed $\mathbf{E} \times \mathbf{B}$ velocity and the density profile. At the peak of the characteristic waveform, the drift current accounts for roughly half of the current to the anode segment at the spoke location.

Using the segmented anode, the current through the spoke has been measured to be over 50% of the anode current, as shown in Fig. 6. Specifically, we find 56% of the total current to be conducted through the spoke with a standard deviation of 13%. Due to variation in the spoke behavior and the possibility of a low amplitude breathing mode, the waveform of the spoke current was determined by averaging over several hundred cycles and averaged across the four segments of the anode. The spoke was identified digitally by finding peaks in the smoothed current, requiring a minimum peak spacing of half the average spoke frequency,

and checking that the anode segment with the peaking current was also collecting the most current of the four segments. The time axis has been normalized to the spoke period, which ranges from 30 μs to 80 μs. During an individual 10 ms data set, the spoke frequency and period is relatively constant (varies 25% of the mean), but operation over several hours can include spoke behavior over the entire frequency range, likely due to changes in thruster temperature and impurity levels. Thus, comparisons across datasets are most insightful if normalized to the spoke period.

The current to the individual segments was found to be highly correlated with the local intensity as observed by the fast camera. The time series of the average brightness over the quarter of the thruster centered on a given segment was compared to the time series of the segment current. The cross correlation was typically 0.9, indicating the strong similarity of the signals, so relying purely upon the segmented anode current proved effective at identifying the spoke location, and the fast camera was not used in electrostatic probe measurements.

The measurement of enhanced cross-field transport represents the first direct measurement of the fluctuation-induced current. Over half of the total current localized to one quarter of the channel area is a significant increase. While the measurements of enhanced current are interesting in themselves, probe measurements were used to investigate the transport mechanism. For the density profile, biased Langmuir probes were used. The probes were biased +48 V above ground to be sufficiently negative compared to the $\sim$ 175 V space potential. A similar averaging process is performed with the ion saturation current traces by identifying the peaks of the spoke current, then taking a time window around the peak and averaging over many cycles. Substituting our measured ion saturation currents as a function of time into Eqn. 1, we are able to solve for the density profile, as shown in Fig. 7 (a). We calculate a density with a mean of 4×10^{11} cm^{-3} and a maximum of 1.4×10^{12} cm^{-3}.

To calculate electron flux due to the rotating spoke, the plasma potential profile of the spoke must be known in addition to the density profile. Emissive probe measurements confirmed an azimuthal electric field across the spoke, in phase with the density fluctuation such that electrons would $\mathbf{E} \times \mathbf{B}$ drift to the anode with a net contribution to the current. The emissive probes were heated until the floating potential would not increase. This was assumed to be 2 T$_e$ below the plasma potential[27]. As the spoke rotates past the probe, the

potential distribution of the rotating spoke is measured. The characteristic waveform of the potential is shown in Fig. 7 (a).

To extrapolate the azimuthal component of the electric field given the potential profile, we assume the spoke velocity and parameters to be constant (on average) as the spoke moves across the emissive probe. An azimuthal electric field may then be calculated by using the spoke velocity to get from a time derivative to a space derivative:

$$E = -\frac{dV}{dx} = -\frac{dV}{dt}(\frac{dx}{dt})^{-1} = -\frac{1}{v_{spoke}}\frac{dV}{dt} \tag{2}$$

Where E is the component of the electric field along the direction of the spoke velocity (azimuthal), V is the space potential of the spoke, and v_{spoke} is the velocity of the spoke. The azimuthal electric field of the spoke as determined using this technique is shown in Fig. 7 (b).

Ultimately, the density and electric field fluctuations are combined to make a simple quantitative estimate of the perturbed current mechanism. The perturbed electric field will cause an axial $E \times B$ drift towards the anode. The drift velocity may then be calculated using the measured azimuthal field and the radial component of the magnetic field, taken to be constant at 760 G, as determined using field simulation software. Indeed, we find a significant drift velocity directed towards the anode when the spoke is present. The drift velocity peaks at 18 km/s, which is fast enough to traverse the 5 mm gap between the measurement location and the anode during the spoke presence. The current caused by this drift may then be estimated as $I_{drift} = ev_d n_e A$, with v_d the drift velocity and A the area of the anode segment. The results are compared with the total enhanced spoke current and are plotted in Fig. 7 (b).

The characteristic electric field, density, and drift current are shown in Fig. 7 overlaid on the single-segment current during a spoke period. The phasing and magnitude reveal the perturbed $E \times B$ drift significantly enhances the cross-field transport. The drift current peaks at 0.26 A within 1 μs of the peak in spoke current, which has a magnitude of 0.48 A. In this finding, we emphasize the phase of the measurement more so than the magnitude. The possibility of fluctuating electron temperature, for instance, increases the uncertainty in the magnitude of the maximum plasma density, whereas the phase information is more clear. The density and electric field peak at similar times. Before and after the peak, however, an offset on the order of 10 μs is present between the drift current and spoke current. Before

and after the spoke, the minimum segment current is 0.1 A while the drift current becomes small and negative due to the reversed direction of the perturbed electric field. It is clear then that additional transport mechanisms are at work within the thruster. On average, since the density is small when the electric field is reversed, there is enhanced drift current. At maximum, the drift current accounts for roughly one third of the total current, and is therefore a key contributor to the transport. We reiterate the approximate nature of the magnitude of the drift current given imprecise density profile measurements. The phase of the density and electric field appear slightly delayed compared to the spoke current. This could be due to the spoke having a tilted profile through the thruster, as past studies have observed a tilt of 15°[14]. Using a spoke velocity of 1.2 km/s, a delay of 10 μs, and the 5 mm separation between the electrostatic probes and the anode, a tilt of 23° is determined using:

$$\tan\theta = \frac{z}{tv_{spoke}} \tag{3}$$

Where θ is the tilt and z the separation between the anode and the probe. While 23° is our best estimate, clear variation in the timing exists in Fig. 7, varying from the estimate by 50% in either direction. We infer a larger spoke tilt on average than Ref.[14].

IV. CONCLUSION

In summary, the cross-field electron transport induced by the rotating spoke was directly measured for the first time using a segmented anode. On average, over 50% of the total current is conducted by the spoke, which is large given the spoke area of one quarter the channel area. The transport mechanism was estimated using electrostatic probes and a drift-induced current model. Given the relative phasing of the density and the potential, approximately half of the spoke current may be explained by this drift current. The remaining spoke current may be from collisional transport and anamalous mechanisms such as electron-wall interactions and fluctuation-induced transport. While the spoke is certainly a macroscopic form of fluctuation-induced transport, the possibility remains for small-scale turbulence which enhances transport beyond the average profiles measured in this paper.

Remaining questions regard the source of the spoke instability. It is not obvious that a m=1 mode should dominate the spoke, and indeed other experiments have revealed higher-mode structure[17]. Moreover, the relatively low speed of the spoke rotation requires explana-

tion. Comparison with the local field values of E = 20 V/cm[29] and B = 850 G indicate the spoke velocity of 2 km/s is 1/10 of the local $E \times B$ velocity of 20 km/s, thus the mechanism for establishing the density and potential perturbation are of theoretical interest. While knowledge of the true $E \times B$ speed is complicated by uncertainty in the local electric field and non-equipotential magnetic field lines, these effects may alter the estimate by a factor of 2 while a difference of a factor of 10 exists. Moreover, the dip in the spoke potential would suggest the local $E \times B$ speed is even larger at the spoke location (estimating the axial electric field as the anode potential minus the spoke potential divided by the separation distance). The common feature of sub-$E \times B$ velocity among the azimuthal perturbation studies[14–18] make it an important emphasis for study. The low velocity has been suggested to be related to the critical ionization velocity[14,16], but the match is inexact and mechanism unconfirmed. It is then of interest to understand the mechanism which determines the velocity and establishes a density perturbation which does not rotate at the E/B speed.

Ultimately, the enhanced transport through the spoke degrades CHT efficiency and understanding the instability mechanism could allow suppression of the spoke mode without the use of the keeper current. For instance, unequal biasing of the segmented anode with opposite phasing of the spoke rotation may suppress the enhanced spoke transport without the onset of worse fluctuations, leading to decreased current and improved CHT efficiency. More fundamentally, the appearance of the perturbation in many thrusters means understanding the rotating spoke is important for basic cross-field transport and perhaps beyond Hall thrusters to more general $E \times B$ devices. Even in the fusion setting, thorough understanding of fluctuation-induced transport and plasma instabilities is critical to optimizing plasma confinement.

The authors would like to thank Jeffrey Parker, Martin Griswold, Jean Carlos Gayoso, and J.P. Sheehan for their assistance during these studies. This work was performed under the support of a DOE - Fusion Energy Sciences Fellowship. This manuscript has been authored by Princeton University and collaborators under Contract Number DE-AC02-09CH11466 with the U. S. Department of Energy with additional support from the Air Force Office of Science Research. The publisher, by accepting this article for publication, acknowledges that the United States Government retains a non-exclusive, paid-up, irrevocable, world-wide license to publish or reproduce the published form of this manuscript, or allow others to do so, for United States Government purposes.

REFERENCES

[1]M. Keidar and I. I. Beilis, IEEE Transactions on Plasma Science **34**, 804 (2006).

[2]J. E. Maggs, T. A. Carter, and R. J. Taylor, Physics of Plasmas **14**, 052507 (2007).

[3]Q. Quraishi, S. Robertson, and B. Walch, Physics of Plasmas **9**, 3264 (2002).

[4]V. V. Zhurin, H. R. Kaufman, and R. S. Robinson, Plasma Sources Science and Technology **8**, R1 (1999).

[5]A. Morozov and A. P. Shubin, Soviet Journal of Plasma Physics **10**, 28 (1984).

[6]J. C. Adam, J. P. Boeuf, N. Dubuit, M. Dudeck, L. Garrigues, *et al.*, Plasma Physics and Controlled Fusion **50**, 124041 (2008).

[7]J. P. Boeuf and L. Garrigues, Journal of Applied Physics **84**, 3541 (1998).

[8]N. B. Meezan, W. A. Hargus Jr., and M. A. Cappelli, Physical Review E **63**, 026410 (2001).

[9]E. Y. Choueiri, Physics of Plasmas **8**, 1411 (2001).

[10]M. J. Burin, G. R. Tynan, G. Y. Antar, N. A. Crocker, and C. Holland, Physics of Plasmas **12**, 052320 (2005).

[11]D. Milligan, D. Gestal, and O. Camino, Journal of the British Interplanetary Society **61**, 466 (2008).

[12]Y. Raitses and N. J. Fisch, Physics of Plasmas **8**, 2579 (2001).

[13]A. Smirnov, Y. Raitses, and N. Fich, Physics of Plasmas **14**, 057106 (2007).

[14]G. S. Janes and R. S. Lowder, The Physics of Fluids **9**, 1115 (1966).

[15]Y. V. Esipchuk, A. I. Morozov, G. N. Tilinin, and A. V. Trofimov, Soviet Physics - Technical Physics **43**, 1466 (1973).

[16]E. Chesta, C. M. Lam, N. B. Meezan, D. P. Schmidt, and M. A. Cappelli, IEEE Transactions on plasma science **29**, 582 (2001).

[17]M. S. McDonald, C. K. Bellant, B. A. S. Pierre, and A. D. Gallimore, JPC Conference 2011(2011).

[18]J. B. Parker, Y. Raitses, and N. J. Fisch, Applied Physics Letters **97**, 091501 (2010).

[19]E. Mobius and R. W. Boswell, Geophysical Research Letters **6**, 29 (1979).

[20]A. W. Smith and M. A. Cappelli, Physics of Plasmas **16**, 073504 (2009).

[21]C. L. Ellison, Y. Raitses, and N. J. Fisch, IEEE Transactions on Plasma Science **Images in Plasmas** (2011).

[22]Y. Raitses, A. Smirnov, and N. J. Fisch, Physics of Plasmas **16**, 057106 (2009).

[23]C. L. Ellison, Y. Raitses, and N. J. Fisch, APS-DPP Conference, Nov. 2010(2010).

[24]A. Smirnov, Y. Raitses, and N. Fich, Journal of Applied Physics **92**, 5673 (2002).

[25]L. Dorf, Y. Raitses, and N. J. Fisch, Applied Physics Letters **84**, 1070 (2004).

[26]L. Dorf, Y. Raitses, and N. J. Fisch, Journal of Applied Physics **97**, 103309 (2005).

[27]J. P. Sheehan, Y. Raitses, N. Hershkowitz, I. Kaganovich, and N. J. Fisch, submitted to Physics of Plasmas **XX**, XX (2011).

[28]L. Dorf, Y. Raitses, and N. J. Fisch, Applied Physics Letters **75**, 1255 (2004).

[29]A. Smirnov, Y. Raitses, and N. Fich, Physics of Plasmas **14**, 057106 (2007).

[30]T. Ito and M. A. Cappelli, Applied Physics Letters **94**, 211501 (2009).

FIGURES

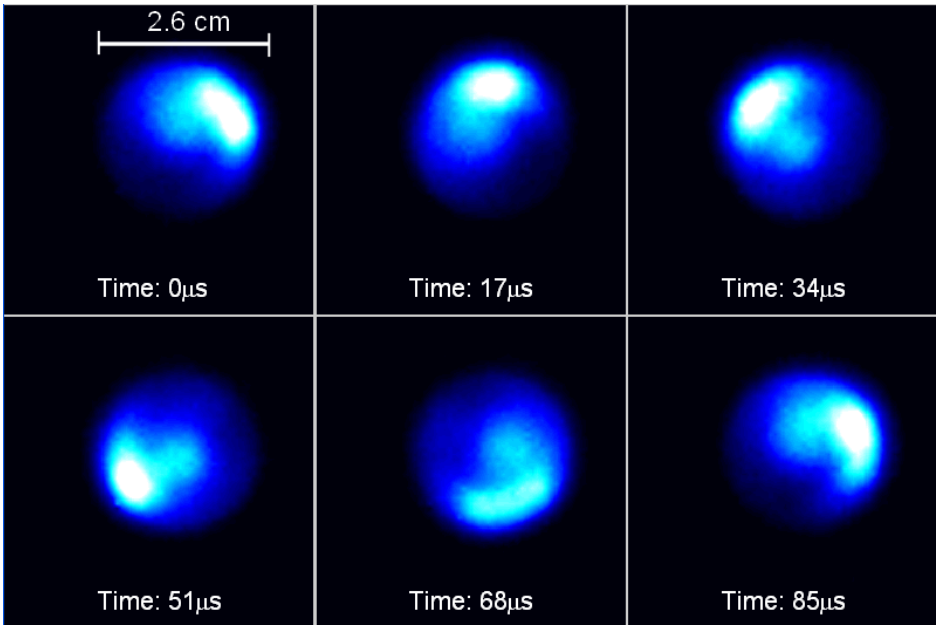

FIG. 1. A series of frames displaying the visible light emission from the rotating spoke instability in the 2.6 cm cylindrical Hall thruster. The 15-35 kHz spoke can be seen to rotate in the counter-clockwise direction, which corresponds to the $\mathbf{E} \times \mathbf{B}$ direction. Color is artificial.

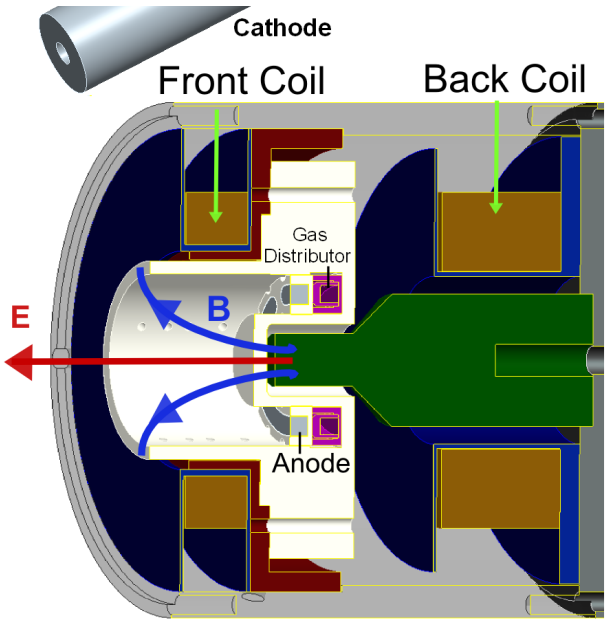

FIG. 2. Cross-section view of a cylindrical Hall thruster. Electrons are magnetized and are confined by a combination of the mirror force and the electric field. Ions are not magnetized and are accelerated by the electric field. Segmented anode shown.

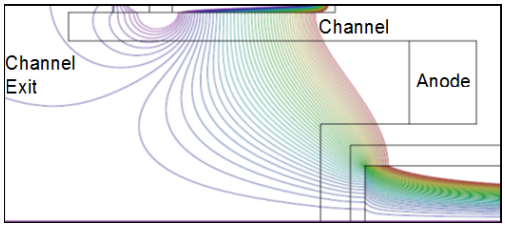

FIG. 3. Simulation of the magnetic field in the cusp configuration, with +2.5 A in the back coils and -2.0 A in the front coils. The enhanced cusp shape forms a stronger mirror field. Image is shown about the axis of symmetry. The maximum magnetic field is 875 Gauss and occurs 6 mm from the anode.

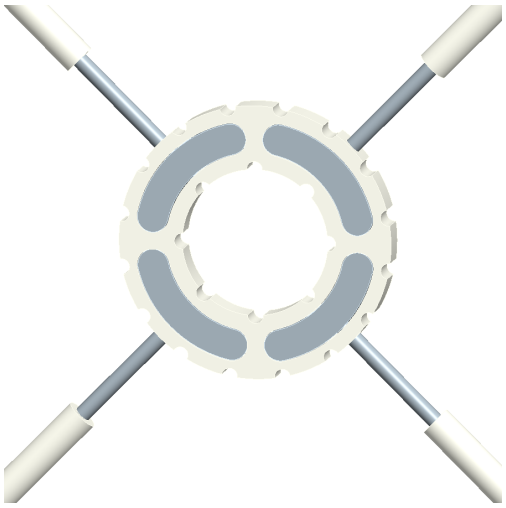

FIG. 4. CAD model of the segmented anode assembly. Boron nitride houses the four stainless steel segments. Threaded rods extrude radially to affix the segments and connect the current path. The 8 internal and 16 external semi-circle holes allow gas distribution.

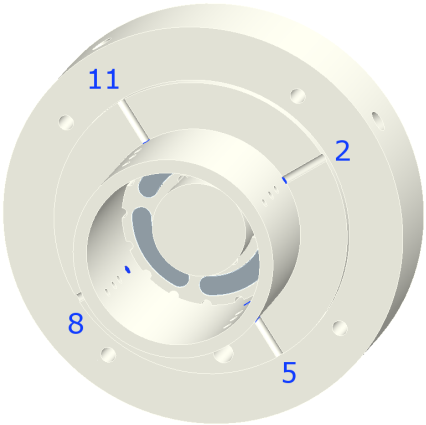

FIG. 5. Probe holes in the ceramic channel are visible in this figure. Only those nearest the anode were used in this experiment, and may be seen by the circular grooves in the face of the channel and blue highlights. Numbers refer to approximate positions on a clock. Emissive probes were placed at positions 2 and 11 while Langmuir probes were placed at 5 and 8.

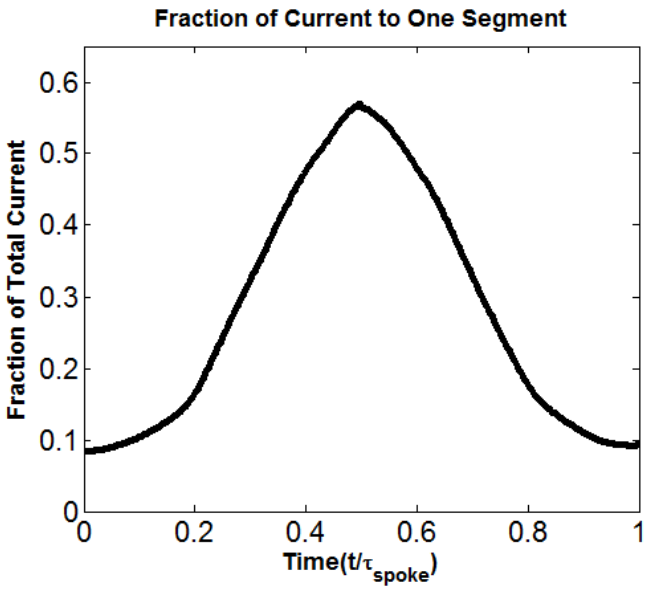

FIG. 6. Characteristic waveform of the current through the rotating spoke to a single segment of the anode. The current rises and falls as the spoke becomes centered over the segment, then passes onto the next. The trace was determined by averaging over several hundred spoke cycles. The time axis is normalized to the spoke period, which ranges from 30 μs to 80 μs. The maximum is 0.57 with a standard deviation of 0.13.

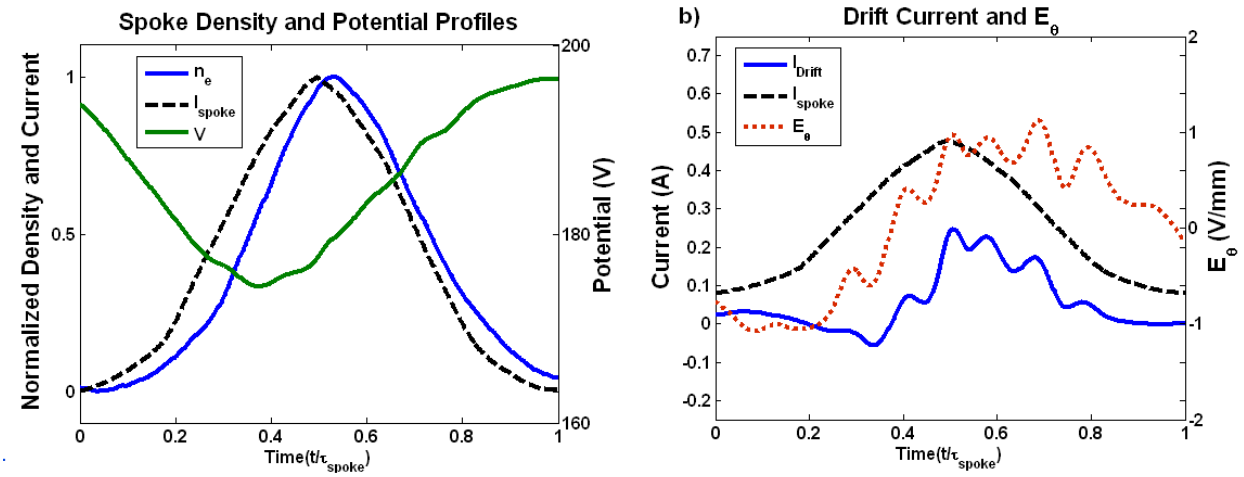

FIG. 7. a) Normalized electron density and potential profile of the rotating spoke. The density has a maximum of 1.4×10^{12} cm^{-3}. b) Calculated drift current and measured azimuthal electric field of the rotating spoke. Spoke current shown to provide reference for the relative phasing.

The Princeton Plasma Physics Laboratory is operated
by Princeton University under contract
with the U.S. Department of Energy.

Information Services
Princeton Plasma Physics Laboratory
P.O. Box 451
Princeton, NJ 08543

Phone: 609-243-2245
Fax: 609-243-2751
e-mail: pppl_info@pppl.gov
Internet Address: http://www.pppl.gov